Site preferences and lattice vibrations of $Nd_6Fe_{13-x}T_xSi$ (T = Co, Ni)*

Huang Tian-Shun(黄天顺)[a)†], Cheng Hai-Xia(成海霞)[b)], Wang Xiao-Xu(王晓旭)[b)c)], Zhang Zhen-Feng(张振峰)[d)], An Zhi-Wei(安志伟)[b)], and Zhang Guo-Hua(张国华)[b)]

[a)] *Electric Engineering Department, Henan Vocatioanl & Technical College, Zhengzhou* 450046, *China*

[b)] *Department of Physics, Beijing University of Science and Technology, Beijing* 100083, *China*

[c)] *Department of Materials Engineering, National Ping Tung University of Technology and Science, Ping-Tung* 91201, *Taiwan, China*

[d)] *The* 20 *Middle School of Beijing, Beijing* 100085, *China*

(Received 12 March 2015; revised manuscript received 16 July 2015; published online 20 August 2015)

The site preferences of the rare earth intermetallics $Nd_6Fe_{13-x}T_xSi$ (T = Co, Ni) are investigated by using interatomic pair potentials which are converted from a lattice-inversion method. Calculation shows that the order of the site preference of Co is 4*d*, 16*k*, 16l_1, and 16l_2 and that of Ni is 16l_2, 16l_1, 16*k*, and 4*d* in $Nd_6Fe_{13-x}T_xSi$. Calculated lattice and positional parameters are found to agree with those reported in the literature. Furthermore, the phonon density of states for $Nd_6Fe_{13-x}T_xSi$ is also evaluated, and a qualitative analysis featuring the coordination and the relevant potentials is carried out.

Keywords: interatomic potentials, site preference, lattice dynamics

PACS: 34.20.Cf, 61.66.Bi, 61.66.Dk **DOI:** 10.1088/1674-1056/24/10/103402

1. Introduction

Over the past several years there have been many studies devoted to rare-earth transition-metal, *R*–M, compounds which contain silicon. Some of these silicon compounds are pseudobinary compounds, such as the $R_2M_{17-x}Si_x$ and $RM_{12-x}Si_x$ compounds,[1–5] and some are true ternary compounds, such as $Nd_6Fe_{13}Si$, in which silicon[6] is required to stabilize the crystal structure. The crystal structure of the $R_6Fe_{13-x}M_{1+x}$ compounds (R = rare earth) was unraveled in 1985 by Sichevich *et al.*[7] They have shown that $La_6Co_{11}Ga_3$ orders in a tetragonal structure with space group I4/*mcm*. Later, Allemand *et al.*[6] showed that $Nd_6Fe_{13}Si$ crystallizes as an ordered variant of this compound. Both structure types are interesting from a technological point of view since their presence as the second phase in NdFeB-permanent magnets enhances the coercivity.[8] Experimentally, there have been studies of replacing Fe atoms in $Nd_6Fe_{13}Si$ by other transition elements, and some of them had promising effects.[9,10] The information about which crystalline site is actually replaced is helpful in understanding the mechanism of the property being changed by substitution. There have been numerous experimental studies devoted to identifying the site occupation.

However, sometimes the experiments do not clearly reveal which sites are substituted. Theoretical study should be a compensatory way to provide helpful information about the site substitution. In this paper, the interatomic potentials acquired by Chen's lattice inversion method are used to investigate the site preferences and lattice constants of these complicated compounds, $Nd_6Fe_{13-x}T_xSi$ (T = Co, Ni). In addition, the phonon densities of states (DOSs) of these rare earth intermetallics are evaluated, from which the corresponding Debye temperatures are obtained.

2. Calculation method

The acquisition of interatomic potentials prepares the groundwork for this research. According to Chen–Möbius' lattice inversion method, the intermetallic pair potentials can be inverted strictly from the cohesive energy curves.[11,12] The methods of obtaining the interatomic pair potentials have been reported in detail.[13–16] In this work, the inverted pair potentials from the cohesive energy are approximately expressed as Morse function

$$\Phi(x) = D_0(\mathrm{e}^{[-\gamma(x/R_0-1)]} - 2\mathrm{e}^{[-(\gamma/2)(x/R_0-1)]}), \qquad (1)$$

where D_0 is the depth of potential, R_0 is the equilibrium distance, and γ is a dimensionless parameter. For clarity, several important potentials are shown in Fig. 1.

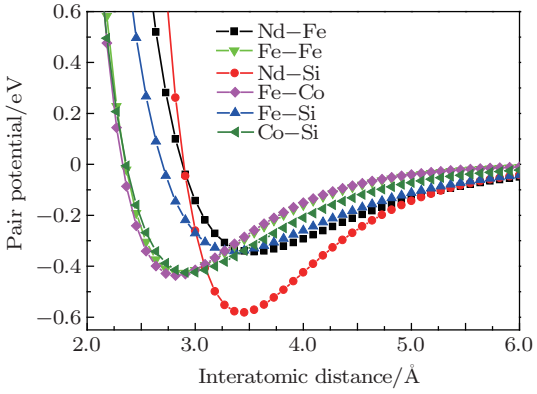


Fig. 1. (color online) Potentials of Nd–Fe, Nd–Si, Fe–Si, Fe–Fe, Fe–Co, and Co–Si.

*Project supported by the National Natural Science Foundation of China (Grant Nos. 11272048 and 50971024) and the National Key Basic Research Program of China (Grant No. 2011CB606401).

†Corresponding author. E-mail: tshuang09@163.com

© 2015 Chinese Physical Society and IOP Publishing Ltd

3. Results and discussion

3.1. Site preference

In this section, we first establish a theoretical structure of $Nd_6Fe_{13}Si$ based on experimental one.[17] Then we study the substitution of Fe sites in this material by Co and Ni by computer simulation, and make comparisons with experiments where possible.

The $Nd_6Fe_{13}Si$-type structure can be described as a multilayer structure in which the layers are perpendicular to the tetragonal c axis. In $Nd_6Fe_{13}Si$ the layers containing neodymium and iron are separated by layers containing only silicon on the 4a sites. The neodymium, which occupies the 8f and 16l sites, is found in layers adjacent to the silicon layer, and the layers of iron 4d, 16k, 16l_1, and 16l_2 sites are sandwiched between the neodymium layers. To illustrate it more clearly, the lattice cell of $Nd_6Fe_{13}Si$ is shown in Fig. 2.

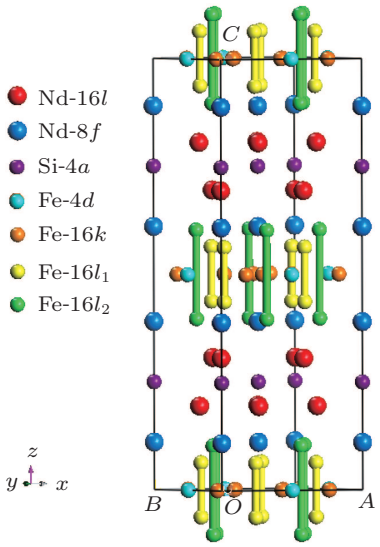


Fig. 2. (color online) Unit cell of $Nd_6Fe_{13}Si$.

According to experimental atomic sites of the model,[17] initial $Nd_6Fe_{13}Si$ structure is constructed with the Accelrys Cerius 2 modeling software. In experiments, it is not easy to substitute elements with various concentrations. Since we have established the uniform and effective pair potential curves, we can numerically compute the effect of element substitutions for arbitrary concentration. We let the element T replace one of the four Fe sites, and optimize the crystal with a conjugate grads method, that is to say, relax the crystal until the cohesive energy reaches a minimum value. The relax system includes $2 \times 2 \times 2 = 8$ crystalline cells. We take the average of 30 sample units for each substitution concentration.

Figure 3 shows the cohesive energy of the $Nd_6Fe_{13-x}T_xSi$ as a function of the T content, and the error bars in the figure represent the ranges of the root mean square errors. For $x \leq 0.34$, the energy is the lowest with Co atoms entering into the 4d sites of the hexagonal structure. Therefore, the Co atoms will preferentially occupy the 4d sites of $Nd_6Fe_{13-x}Co_xSi$ compounds. For $Nd_6Fe_{13-x}Ni_xSi$, Ni atoms entering into the 16l_2 sites have the lowest energy. So Ni atoms should prefer the 16l_2 sites with the space group $I4/mcm$ for $Nd_6Fe_{13-x}Ni_xSi$ compounds. The calculated results show that the preferential occupation sequence for Co is 4d, 16k, 16l_1, and 16l_2, and that for Ni is 16l_2, 16l_1, 16k, and 4d in $Nd_6Fe_{13-x}T_xSi$.

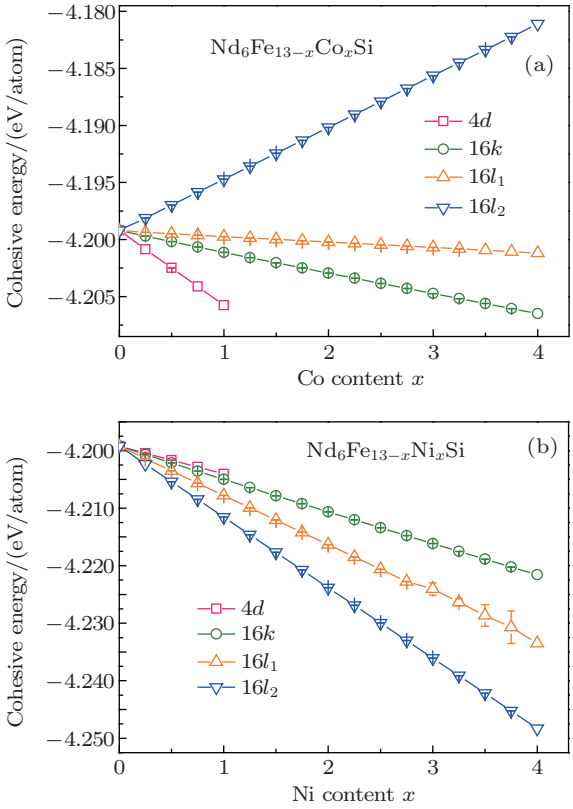


Fig. 3. (color online) The calculated values of cohesive energy of $Nd_6Fe_{13-x}T_xSi$ (T = Co, Ni) compounds.

Table 1. Lattice parameters a and c of $Nd_6Fe_{13-x}T_xSi$ in unit Å.

Compounds	Temperature/K	a (exp.)	a (cal.)	c (exp.)	c (cal.)	Ref.
$Nd_6Fe_{13}Si$	0	8.047(2)	8.090	22.809(3)	22.353	[9]
	17	8.0388(1)	8.090	22.709(1)	22.353	[17]
	295	8.0452(1)	8.106	22.772(1)	22.369	[17]
$Nd_6Fe_{12}CoSi$	0	8.038(3)	8.080	22.776(2)	22.359	[9]
$Nd_6Fe_{11}Co_2Si$	0		8.076		22.291	
	600		8.089		22.312	
$Nd_6Fe_{11}Ni_2Si$	0		8.069		22.298	

According to the results for the occupancy behaviors of T, the lattice parameters of the $Nd_6Fe_{13-x}T_xSi$ are calculated when T atoms are in 4d or 16l_2 sites. Table 1 shows the results of $Nd_6Fe_{13-x}T_xSi$ obtained from both the experiments[9,17] and calculation. Atomic parameters have also been investigated based on the inverted pair potentials (Table 2). The calculated atomic parameters of $Nd_6Fe_{13-x}T_xSi$ are close to experimental results.[17] The differences between the experimental and calculated lattice and positional parameters are at most 2.00%, which is quite acceptable.

Table 2. Positional parameters in $Nd_6Fe_{13}Si$ at 17 K and 295 K.

Atomic parameters	x/a, y/b, z/c (17 K)		x/a, y/b, z/c (295 K)	
	Exp.[17]	Cal.	Exp.[17]	Cal.
Nd, 8*f*	0, 0, 0.1106(3)	0, 0, 0.1101	0, 0, 0.1115(3)	0, 0, 0.1100
Nd, 16*l*	0.1671(4), 0.6671(4), 0.1906(2)	0.1607, 0.6601, 0.1942	0.1663(4), 0.6663(4), 0.1903(2)	0.1604, 0.6600, 0.1945
Fe, 4*d*	0, 0.5, 0	0, 0.5, 0	0, 0.5, 0	0, 0.5, 0
Fe, 16*k*	0.0678(5), 0.2101(3), 0	0.0667, 0.2064, 0	0.0673(5), 0.2082(3), 0	0.0667, 0.2060, 0
Fe, 16l_1	0.1777(3), 0.6777(3), 0.0614(2)	0.1755, 0.6761, 0.0631	0.1783(4), 0.6783(4), 0.0614(2)	0.1752, 0.6760, 0.0630
Fe, 16l_2	0.3876(3), 0.8876(3), 0.0974(2)	0.3807, 0.8801, 0.1029	0.3876(4), 0.8878(4), 0.0974(2)	0.3799, 0.8796, 0.1028
Si, 4*a*	0, 0, 0.25	0, 0, 0.25	0, 0, 0.25	0, 0, 0.25

Furthermore, the structural property is to be simulated by the high temperature disturbance test with molecular dynamics to check the lattice constants and phase stability at high temperature. We thus perform molecular dynamics simulations at constant pressure and temperature (NPT, where N denotes the number of particles, P the pressure, and T the temperature). For constant-NPT molecular dynamics the temperature and pressure are kept constant with using an extended system with a thermostat and barostat relaxation time of 0.1 ps. The simulation temperature range is 0 K–900 K. For each temperature and at 1 atm (1 atom = 1.01325×10^5 Pa), pressure calculations are performed for 5×10^4 steps in time steps of 2.0×10^{-15} s. After equilibrium is reached, the crystal symmetry remains in the initial $I4/mcm$ space group. The lattice and positional parameters for $Nd_6Fe_{13-x}T_xSi$ can also be obtained and are given in Tables 1 and 2. From Tables 1 and 2, one can see that our results for $Nd_6Fe_{13-x}T_xSi$ at difference temperatures are in agreement with experimental results,[17] which means that the applicability of the present interatomic potential is well proven by demonstrations.

3.2. Lattice dynamic simulations

Starting with the effective interatomic potentials and lattice dynamics theory, we calculate the total DOS and the partial DOS projected to different elements in $Nd_6Fe_{13-x}T_xSi$. The calculated results are shown in Fig. 4. The DOS of Fig. 4 is calculated by adding up 936 k points in 1/8 the first Brillouin zone of a simple tetragonal lattice. The cut-off distance

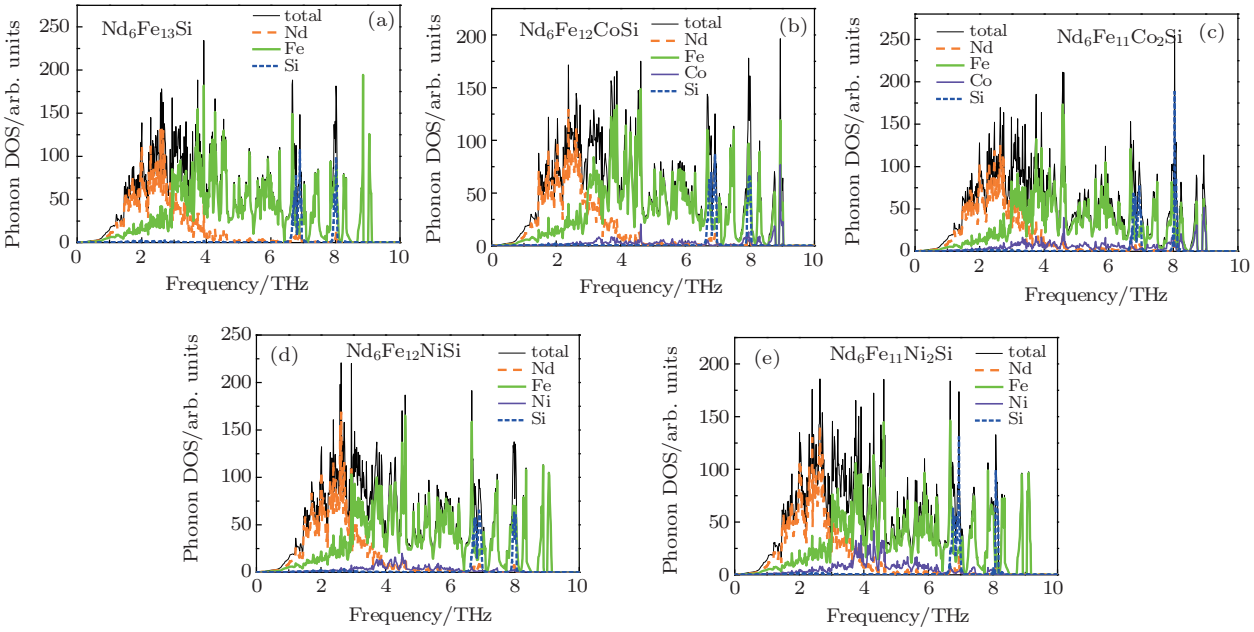


Fig. 4. (color online) Phonon DOSs of $Nd_6Fe_{13-x}T_xSi$ (T = Co, Ni) compounds.

of force constants is set at 6 Å. It is estimated that the cut-off frequencies of the vibrational modes are 9.12 ($Nd_6Fe_{13}Si$), 9.02 ($Nd_6Fe_{12}CoSi$), 9.01 ($Nd_6Fe_{11}Co_2Si$), 9.14 ($Nd_6Fe_{12}NiSi$), and 9.17 ($Nd_6Fe_{11}Co_2Si$) THz, respectively. From the partial DOS, it can be inferred that the vibrational modes above 3.00 THz are mostly excited by Fe. Rare earth Nd atoms contribute a major part to the modes with lower frequencies. The Si atom only contributes to three optically localized modes around 6.8, 7.0, and 8.0 THz.

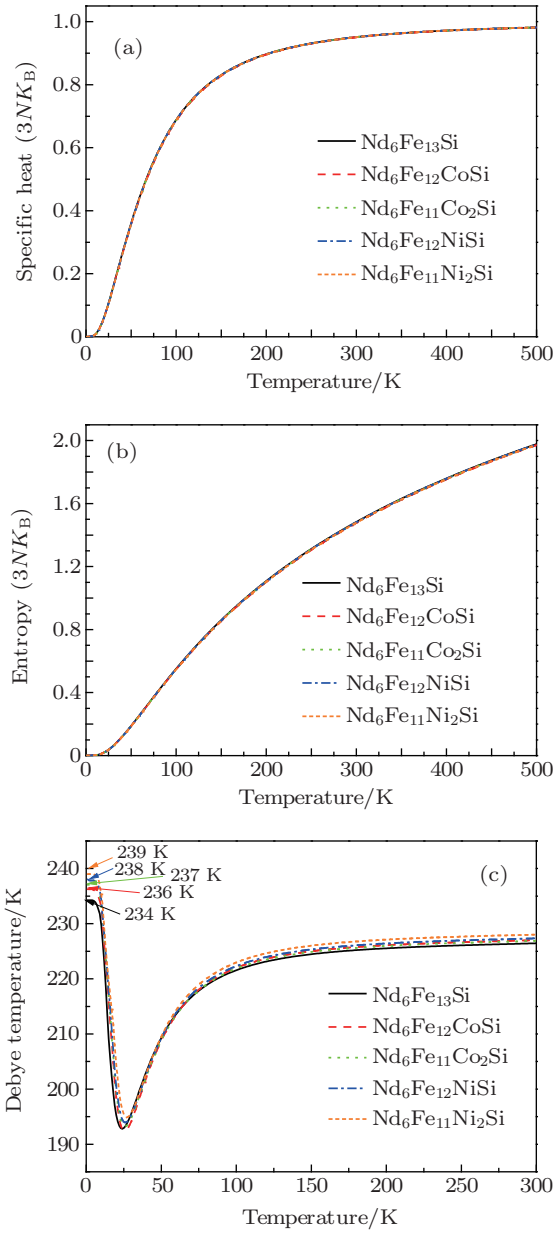


Fig. 5. (color online) Calculated values of specific heat, vibrational entropy, and Debye temperature of $Nd_6Fe_{13-x}T_xSi$ (T = Co, Ni) compounds.

In this work, the localized modes are analyzed qualitatively from interatomic potentials in Fig. 1. We take $Nd_6Fe_{11}Co_2Si$ for example. Since the curve $\Phi_{Nd-Si}(r)$ is deep and narrow, Nd atoms react quite strongly with the nearest-neighbor Si atoms. The mass of the Nd atom is approximately five times that of the Si atom, so the Nd atoms are assumed to be motionless relative to the Si atoms. Then the Si atoms are restricted by the Nd atoms in the 'potential well' $\Phi_{Nd-Si}(r)$ and excite the local modes which correspond to the higher frequencies. For Nd atoms, they only contribute to lower frequency vibrations in the Nd-Si 'potential well' because of their large atomic mass. The distances between Fe ($16l_2$) and its nearest Fe atoms at the Fe ($16k$) or ($16l_1$) sites are within 2.501 Å–2.711 Å. From Fig. 1, it can be seen that the interactions between Fe and Fe at these distances are very strong, which results in a restriction that causes Fe to vibrate at the total frequency. As shown in Fig. 1, the Fe–Fe interaction is nearly the Co–Fe interaction. Hence, the frequency modes of the Co are almost the same as those of the Fe in shape, but the amplitudes are much smaller because the quantity of ternary elements is small.

Figure 5 gives the calculated values of lattice specific heat and vibrational entropy of $Nd_6Fe_{13-x}T_xSi$. The figure clearly shows that the variations of specific heat and entropy with temperature for the ternary systems do not show any anomaly. The calculated Debye temperature of $Sm_2Fe_{15}Mn_2$ is also shown in Fig. 5. The values of $Nd_6Fe_{13}Si$, $Nd_6Fe_{12}CoSi$, $Nd_6Fe_{11}Co_2Si$, $Nd_6Fe_{12}NiSi$ and $Nd_6Fe_{11}Co_2Si$ are 234, 236, 237, 238, and 239 K near 0 K, respectively. The changes of Debye temperature are relatively small when the T atoms substitute Fe atoms in the $Nd_6Fe_{13}Si$ compound.

4. Summary

In this work, the site occupancies of Fe and Co in $Nd_6Fe_{13}Si$ are investigated by interatomic potentials which are converted from the Chen–Möbius' lattice-inversion method. The calculated cohesive energy of $Nd_6Fe_{13-x}T_xSi$ shows that the preferential orders of T = Co and Ni are $4d$, $16k$, $16l_1$, $16l_2$, and $16l_2$, $16l_1$, $16k$, $4d$, respectively. The calculated lattice and positional parameters are in good agreement with observed results from the literature. In addition, we utilize the inversion pair potentials to evaluate the phonon density of states of $Nd_6Fe_{13-x}T_xSi$, and obtain its specific heat, vibrational entropy and Debye temperature.

References

[1] Long G J, Marasinghe G K, Mishra S, Pringle O A, Grandjean F, Yelon W B, Pourarian F and Isnard O 1993 *Solid State Commun.* **88** 761
[2] Artigas M, Fruchart D, Isnard O, Miraglia S and Soubeyroux J L 1999 *J. Alloys Compd.* **291** 282
[3] Isnard O and Buschow K H J 1997 *J. Alloys Compd.* **267** 50
[4] Buschow K H J 1988 *J. Appl. Phys.* **63** 3130
[5] Solzi M, Pareti L, Moze O and David W I F 1988 *J. Appl. Phys.* **64** 5084

[6] Allemand J, Letant A, Moreau J M, Nozières J P and Perrier de la Bâthie R 1990 *J. Less-Common Metal* **166** 73
[7] Sichevich O M, Lapunova R V, Soboley A N, Grin Yu N and Yarmulek Ya P 1985 *Sov. Phys. Crystallogr.* **30** 627
[8] Schrey P and Velicescu M 1991 *J. Magn. Magn. Mater.* **101** 417
[9] Iranmanesh P, Tajabor N, Rezaee Roknabadi N, Pourarian F and Brück E 2011 *Intermetallics* **19** 682
[10] Iranmanesh P, Tajabor N and Pourarian F 2013 *Intermetallics* **42** 180
[11] Chen N X and Ren G B 1992 *Phys. Rev. B* **45** 8177
[12] Chen N X, Chen Z D and Wei Y C 1997 *Phys. Rev. E* **55** R5
[13] Cheng H X, Wang X X, Hu Y W, Zhang G H, Shen J, Qian P, Chen N X 2015 *J. Solid State Chem.* **224** 7
[14] Wang X X, Qian P, Zhang Z F, Liu Y, Shen J and Chen N X 2013 *Intermetallics* **42** 112e119
[15] Li J C, Qian P, Zhang Z F, Yuan X J, Wang Y W, Shen J and Chen N X 2013 *J. Solid State Chem.* **201** 250
[16] Qian P, Hu Q Y, Shen J, Feng Y, Pan H Y and Hu P 2010 *Model. Simul. Mater. Sci. Eng.* **18** 045002
[17] Isnard O, Long G J, Hautot D, Buschow K H J and Grandjean F 2002 *J. Phys.: Condens. Matter* **14** 12391